

**Strong Coupling Hot Paper**How to cite: *Angew. Chem. Int. Ed.* **2021**, 60, 5712–5717

International Edition: doi.org/10.1002/anie.202013465

German Edition: doi.org/10.1002/ange.202013465

Modifying Woodward–Hoffmann Stereoselectivity Under Vibrational Strong Coupling

Abhijit Sau⁺, Kalaivanan Nagarajan⁺, Bianca Patrahau, Lucas Lethuillier-Karl, Robrecht M. A. Vergauwe, Anoop Thomas, Joseph Moran,* Cyriaque Genet,* and Thomas W. Ebbesen*

Abstract: Vibrational strong coupling (VSC) has recently been shown to change the rate and chemoselectivity of ground-state chemical reactions via the formation of light–matter hybrid polaritonic states. However, the observation that vibrational-mode symmetry has a large influence on charge-transfer reactions under VSC suggests that symmetry considerations could be used to control other types of chemical selectivity through VSC. Here, we show that VSC influences the stereoselectivity of the thermal electrocyclic ring opening of a cyclobutene derivative, a reaction which follows the Woodward–Hoffmann rules. The direction of the change in stereoselectivity depends on the vibrational mode that is coupled, as do changes in rate and reaction thermodynamics. These results on pericyclic reactions confirm that symmetry plays a key role in chemistry under VSC.

The Woodward–Hoffmann (WH) rules elaborated in the 1960's epitomizes the importance of symmetry in chemical reactivity.^[1–6] In essence, the conservation of orbital symmetry between reactants and products affect the reaction landscape and thereby the products that are favoured. In ideal cases, such as for *cis*-3,4-disubstituted cyclobutene, the products that are forbidden in the ground states are allowed in the excited state and vice-versa: *cis*-3,4-disubstituted cyclobutene undergoes conrotatory electrocyclic ring opening under thermal conditions to form *cis-trans*-1,3-butadiene, while under photochemical condition, *trans*, *trans*-1,3-butadiene is obtained through the disrotatory pathway, as illustrated in Figure 1 a. However, in most cases, a mixture of products is obtained due to effects that mitigate the symmetry-based outcome, such as secondary effects of substituents, even if overall the WH rules are followed.^[2–6]

Chemistry under strong coupling has received much attention since the first demonstration of a modified chemical landscape.^[7–34] Recently, we reported that vibrational symmetry plays a key role in modifying the charge-transfer complexation equilibrium between I₂ and mesitylene under vibrational strong coupling (VSC).^[12] To further explore the

role of symmetry under VSC, we have chosen the well-studied thermal electrocyclic ring-opening of cyclobutene into butadiene, where the reaction path can be predicted by the principle of orbital symmetry conservation according to the WH rules. Among the various cyclobutene derivatives reported for this kind of reaction, we have synthesised cyclobutene-*cis*-3,4-dimethylcarboxylate (CB), which is suitable for studies under VSC. As expected from the WH rules,^[1] the molecule under study undergoes thermal ring-opening at 90°C to yield mostly the corresponding symmetry-allowed *cis-trans* product, but also some symmetry-forbidden *trans-trans* 1,3-butadiene product. The formation of symmetry-forbidden *trans-trans* butadiene can be attributed to secondary orbital interaction from the carbonyl group, which reduces the activation energy of the disrotatory transition state.^[3–6] In addition, it is a liquid at room temperature, the reaction is monomolecular and gives no products other than to those expected from the WH rules, all features that simplify the study.

Vibrational strong coupling (Figure 1 b) is achieved by placing the molecular solution inside a Fabry-Perot optical cavity, which is tuned to have a mode in resonance with a selected vibrational mode of the molecule (Figure 1 c). When the conditions for strong coupling are satisfied, the molecular transition splits into two new hybrid states known as P⁺ and P[−], separated by a Rabi splitting energy ($\hbar\Omega_R$). The strength of strong coupling is denoted by the Rabi splitting energy, which is proportional to the transition dipole moment of the vibration and square root of the concentration of the coupled molecules inside the cavity. VSC occurs in the dark due to the coupling of the zero-point energy of the cavity mode with that of the vibrational transition.^[9]

The Fabry-Perot cavity was fabricated by separating two parallel Au (10 nm) mirror-coated ZnSe substrates with a 6 μm Mylar spacer, and having a hollow channel designed to inject the liquid sample. Such cavities will generate many resonances separated the free spectral range or FSR and one of them needs to be tuned to a vibration (Figure S1,

[*] A. Sau,^[‡] K. Nagarajan,^[‡] B. Patrahau, L. Lethuillier-Karl, R. M. A. Vergauwe, A. Thomas, J. Moran, C. Genet, T. W. Ebbesen
University of Strasbourg, CNRS, ISIS & icFRC
67000 Strasbourg (France)
E-mail: moran@unistra.fr
genet@unistra.fr
ebbesen@unistra.fr

[‡] These authors contributed equally to this work.

Supporting information and the ORCID identification number(s) for the author(s) of this article can be found under:
<https://doi.org/10.1002/anie.202013465>.

© 2020 The Authors. Angewandte Chemie International Edition published by Wiley-VCH GmbH. This is an open access article under the terms of the Creative Commons Attribution Non-Commercial NoDerivs License, which permits use and distribution in any medium, provided the original work is properly cited, the use is non-commercial and no modifications or adaptations are made.

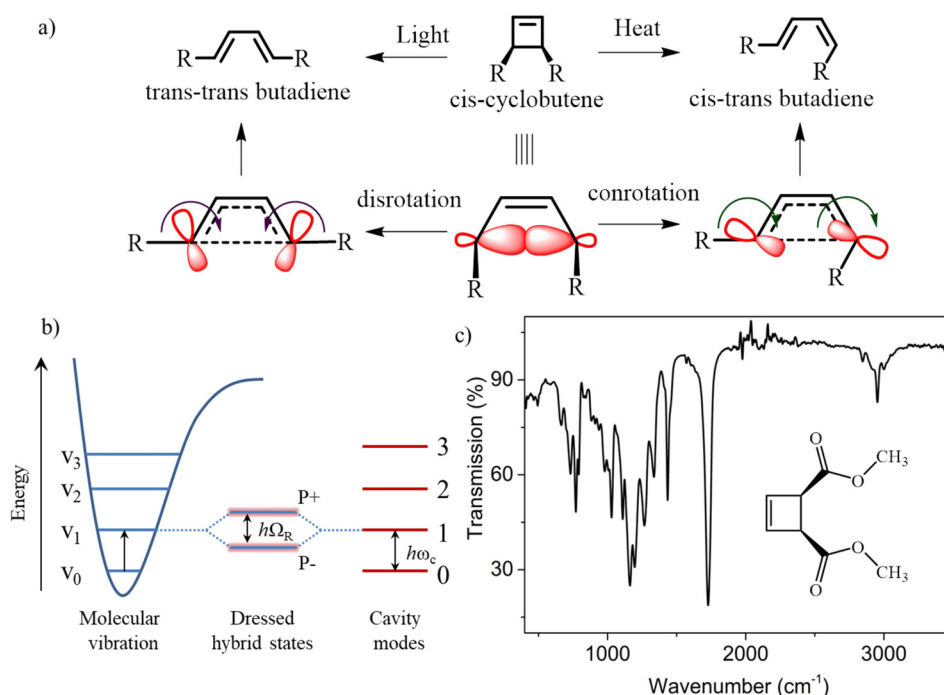


Figure 1. a) Electrocyclic ring-opening reaction of *cis*-3,4-disubstituted cyclobutene which undergoes conrotation under thermal condition to form *cis*-trans butadiene and disrotation in the presence of light to give *trans*-*trans* butadiene; b) Schematic representation of vibrational strong coupling between the molecular vibrational transition and Fabry-Perot cavity mode; c) FT-IR spectra of cyclobutene-*cis*-3,4-dimethylcarboxylate, with inset showing the molecular structure.

Supporting Information). To prevent the reaction mixture from coming in contact with the metal surface, 200 nm of SiO_x was sputtered on top of the Au. For the so-called non-cavity condition, the same SiO_x coated windows were used but without the Au coating. Electrocyclic ring-opening of CB was performed by heating the sample at 90°C for two hours (Figure 2a). To begin, we followed the reaction under non-cavity conditions (Figure S2, Supporting Information). Neat CB was injected into the preheated chamber at 90°C and the reaction was monitored in the FT-IR (Figure 2b). The first-order nature of the reaction was confirmed by the exponential growth of the peak at 1602 cm^{-1} , which corresponds to the $\text{C}=\text{C}$ stretching mode of the butadiene derivative (Figure S3a, Supporting Information). After two hours, the reaction mixture was allowed to cool to room temperature (RT) and dissolved in CDCl_3 to perform the $^1\text{H-NMR}$ measurement. The $^1\text{H-NMR}$ spectrum shows the formation of the symmetry-allowed *cis*-trans butadiene and the symmetry-forbidden *trans*-*trans* derivative, along with the unreacted starting material CB (Figure 2e). The *trans*-*trans* butadiene is characterised by the signals **a** and **b**, whereas the *cis*-trans derivative is identified by the signals **c**, **d**, **e** and **f**, as shown in Figure 2. As predicted by the WH rules, the symmetry-allowed *cis*-trans butadiene is obtained as the major product (92 %) while the symmetry-forbidden *trans*-*trans* derivative is present only with a 8 % yield. This leads to a ratio between symmetry-allowed conrotatory (*cis*-*trans*) vs. symmetry-forbidden disrotatory (*trans*-*trans*) product ratio of 12.7 ± 0.5 . No other products or intermediates were observed in the NMR spectra. The overall reaction rate (k_{obs}) at 90°C under

non-cavity conditions was 0.0120 min^{-1} (Figure 2h). The formation of symmetry-forbidden *trans*-*trans* butadiene product is attributed to the secondary orbital interactions arising from the carbonyl groups at C3 and C4 of cyclobutene derivative CB.^[3-6]

To perform the reaction under VSC, the FSR of Fabry-Perot cavities were carefully tuned at 90°C to have a mode to couple either carbonyl stretching band at 1740 cm^{-1} or the in-plane C-H bending at 1436 cm^{-1} . Cavity tuning is easily performed by adjusting the screws that hold the assembly together, as detailed in the Supporting Information (Figure S1, Supporting Information). As with the non-cavity experiment, the cavity assembly was equilibrated at 90°C for two hours before injecting the sample.

In a first set of experiments, the 5th mode of the Fabry-Perot cavity was tuned to the $\text{C}=\text{O}$ stretching mode of CB (Figure 2c) at 1740 cm^{-1} at 90°C . Neat CB was injected and the reaction progress was monitored by FT-IR. The appearance of equally spaced P+ and P- with a Rabi splitting of 160 cm^{-1} , corresponding to the molecular transition at 1740 cm^{-1} , confirms the strong coupling. The other peaks in Figure 2c are the 4th and 6th cavity modes and are not interacting with any vibrations. The kinetics of the reaction was followed by monitoring the shift in the higher order cavity modes, which reflects the difference in refractive index of the reactant and products (Figure S3, Supporting Information). It should be noted that both the reactant and the products have the same $\text{C}=\text{O}$ group and therefore as the reaction proceeds the system remains coupled and the Rabi splitting hardly changes. Under VSC of $\text{C}=\text{O}$ stretching, the overall reaction rate (k_{obs}) was 0.0080 min^{-1} . After two hours, the reaction mixture was allowed to cool down to RT and the products were quantified by $^1\text{H-NMR}$ (Figure 2f). Surprisingly, we observed significant reduction in the symmetry-forbidden *trans*-*trans* butadiene derivative (1.5 %) when compared to the non-cavity condition (8 %, Figure 2i). This leads to a ratio between the symmetry-allowed and the symmetry-forbidden products of 28 ± 2 under VSC of the $\text{C}=\text{O}$ stretching mode. As detailed in the Supporting Information, only $\approx 60\%$ area of the Fabry-Perot cavity is homogeneous and tuned under VSC. By incorporating the area correction, the ratio of *cis*-*trans* to *trans*-*trans* butadiene is actually 38 ± 2 (Table 1). In other words, coupling the $\text{C}=\text{O}$ stretching mode increases the selectivity for the symmetry-allowed product.

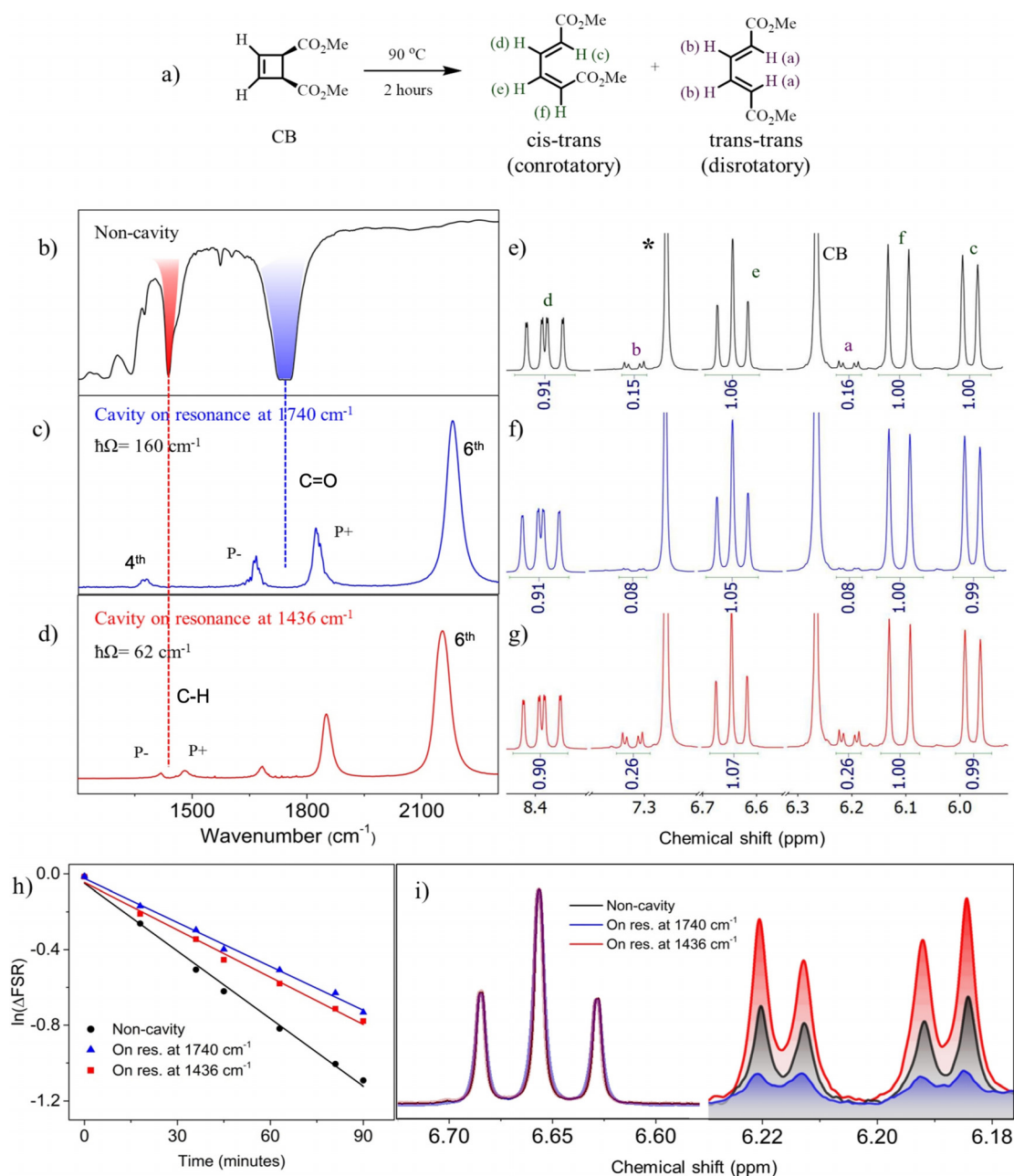


Figure 2. a) Electrocyclic ring opening reaction of cyclobutene-cis-3,4-dimethylcarboxylate (CB) under thermal conditions. FT-IR spectra in transmission mode of b) non-cavity conditions, c) under VSC of the C=O stretching mode (1740 cm^{-1}) and d) under VSC of the C-H bending mode (1436 cm^{-1}). e), f) and g) $^1\text{H-NMR}$ spectra showing alkenyl proton signals of cis-trans and trans-trans butadiene products along with the unreacted cyclobutene starting material obtained, respectively from non-cavity conditions, VSC at 1740 cm^{-1} and VSC at 1436 cm^{-1} . Note that the ^1H signal labelled * is from CDCl_3 and CB is from unreacted starting material. h) Observed kinetics (k_{obs}) of the reaction under non-cavity (black circle) and under VSC conditions (C=O, blue triangles and C-H, red square). i) Superimposed $^1\text{H-NMR}$ signals normalised to the cis-trans signal e showing the change in the yield of the disrotation product trans-trans (signal a).

In a second series of experiments, we coupled the cyclobutene ring C-H in-plane bending mode (Figure 2d), which overlaps with the strong CH_3 deformation modes at 1436 cm^{-1} . After injecting the neat sample into the equilibrated cavity at 90°C , FT-IR spectra show P+ and P- with a Rabi splitting of 62 cm^{-1} with the 4th mode of the cavity. It should be noted that an apparent splitting appears between the 5th mode and the C=O stretching mode but closer analysis

shows that it is detuned by 60 cm^{-1} . It is now well-known that at such detuning, there is no strong coupling effect on the chemistry.^[12,15,16,22,23] Again, after two hours, the reaction mixture was analysed by $^1\text{H-NMR}$. Similar to VSC of C=O stretching mode, the overall reaction rate (k_{obs}) was found to be 0.0083 min^{-1} . Interestingly, we observed a significant enhancement in the formation of symmetry-forbidden trans-trans butadiene (15%) when compared to the non-cavity

Table 1: Cis-trans to trans-trans product ratio (conrotation/disrotation) obtained from $^1\text{H-NMR}$ measurements of electrocyclic ring opening of CB at 90°C in non-cavity and cavity tuned to different vibrational modes. Relative Gibbs free energy change ($\Delta\Delta G^\ddagger$) between the con and disrotatory transition states are obtained from the product ratio using Equation (3).

Experiment	cis-trans/ trans- trans	$\Delta\Delta G^\ddagger$ [kJ mol $^{-1}$]
Non-cavity	12.7 ± 0.5	7.7 ± 0.2
Cavity off resonance	12.4 ± 0.5	7.6 ± 0.2
Cavity on resonance		
C=O stretching mode (1740 cm^{-1})	38.0 ± 2	11.0 ± 0.5
C-H bending mode, in-plane (1436 cm^{-1})	5.0 ± 1	4.9 ± 0.5

condition (Figure 2g and i). This results in a symmetry-allowed vs. symmetry forbidden product ratio of 5 ± 1 , after correcting the values for the tuned area (Table 1).

As a final reference, similar experiments were performed at off-resonance condition (Figure S4, Supporting Information) where none of the cavity modes are strongly coupled with any of the molecular vibrations. The mere presence of cavity modes in the off-resonance experiments did not show any modification in the product ratio (Table 1), which demonstrates the importance of strong coupling between the cavity mode and the molecular transition to observe the changes in the reaction.

Individual rate constants for the symmetry-allowed conrotatory (k_{con}) and symmetry-forbidden disrotatory (k_{dis}) ring-openings were estimated from the observed rate constant (k_{obs}) of the reaction (Figure 2h) and the product ratio, by combining Equations (1) and (2):

$$k_{\text{con}} + k_{\text{dis}} = k_{\text{obs}} \quad (1)$$

$$\frac{k_{\text{con}}}{k_{\text{dis}}} = \frac{[\text{cis} - \text{trans}]}{[\text{trans} - \text{trans}]} \quad (2)$$

The rate of formation of cis-trans and trans-trans butadiene under non-cavity conditions at 90°C was 0.011 min^{-1} and 0.001 min^{-1} respectively. Under VSC, k_{con} and k_{dis} varies depending on the coupled vibration and the values are given in the Supporting Information (Table S1).

The difference between the free energies of activation of the symmetry-allowed conrotation and symmetry-forbidden disrotation could be calculated from the product ratio by using the following equation, and the results are shown in the Table 1.

$$\Delta\Delta G^\ddagger = RT \ln \frac{[\text{cis} - \text{trans}]}{[\text{trans} - \text{trans}]} \quad (3)$$

In non-cavity conditions, the average free energy change between con- and disrotatory transition states of CB at 90°C is $7.6 \pm 0.2 \text{ kJ mol}^{-1}$, which is much lower when compared to cis-3,4-dimethylcyclobutene ($35\text{--}40 \text{ kJ mol}^{-1}$).^[2] This significant reduction in the $\Delta\Delta G^\ddagger$ can be attributed to the

stabilisation of the disrotatory transition state through secondary orbital interactions with the carbonyl group.^[3-6] VSC of the C=O stretching mode exhibits increased $\Delta\Delta G^\ddagger$ ($11 \pm 0.5 \text{ kJ mol}^{-1}$), resulting in reduced trans-trans product formation, which presumably occurs due to the perturbation of the secondary orbital interaction of the C=O with the cyclobutene ring. On the other hand, VSC on C-H bending shows decreased $\Delta\Delta G^\ddagger$ ($4.9 \pm 0.5 \text{ kJ mol}^{-1}$), which enhances the symmetry-forbidden trans-trans product.

Such modifications can be interpreted by looking at the additional symmetry constraints that VSC puts on the orbital correlation diagram. Let us start with the case of VSC involving the in-plane C-H bending mode. The cavity mode strongly coupled to the molecules puts the orbitals in-phase with respect to the intracavity field, and thus forces the phases of the newly formed p orbitals to remain symmetric with respect to the mirror plane of the cis-cyclobutene moiety (Figure 1a). Such symmetries are compatible with the electrocyclic ring-opening through a disrotation, explaining why VSC on C-H bending favours disrotatory processes and increases k_{dis} in the reaction path.

To understand the effects of VSC of the C=O stretching mode, it should be recalled the peculiar role played by the carbonyl groups in the ring-opening process.^[3-6] It mediates secondary, but efficient, orbital interactions with the cyclobutene ring and thereby affecting the WH rules.

As shown in Figure 3, the trans-trans isomer has divergent carbonyl groups while the cis-trans isomer displays carbonyl groups closely aligned. Considering that the single-mode intracavity electric field E_{cav} puts the dipoles in-phase under VSC, these two configurations lead to two resulting collective dipoles D that are expected to yield different contributions to the C=O dipolar coupling DE_{cav} . The well-aligned carbonyl groups of the cis-trans isomer resulting in the larger resulting permanent dipole moment should increase the coupling strength with the intracavity electric field relative to the trans-trans isomer. We can then anticipate that under VSC, the electrocyclic ring-opening is driven accordingly: the conrotation path leads to the cis-trans isomer that favours VSC over the disrotation path. From a thermodynamic viewpoint, this corresponds to an increased stabilization of the conrotatory transition state.

The thermodynamics of the electrocyclic ring-opening reaction under VSC of both the C=O and the C-H vibrations were determined by measuring the reaction rate as a function of temperature (Figure S5, Supporting Information). The

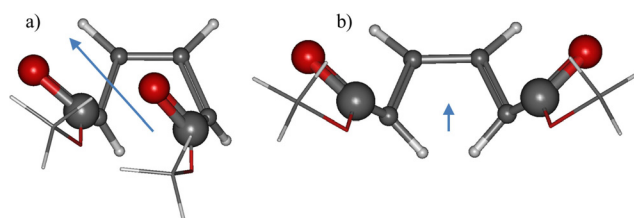


Figure 3. Relative orientation of carbonyl groups in the transition state expected in a) symmetry allowed conrotation and b) symmetry forbidden disrotation.

Table 2: Thermodynamic parameters in non-cavity and cavity conditions tuned to different vibrational modes. ΔG^\ddagger values are given for 90 °C.

Experiment	ΔH^\ddagger [kJ mol ⁻¹]		ΔS^\ddagger [J mol ⁻¹ K ⁻¹]		ΔG^\ddagger [kJ mol ⁻¹]	
	cis-trans	trans-trans	cis-trans	trans-trans	cis-trans	trans-trans
Non-cavity	93	92	5	-18	91	99
C=O coupling	79	82	-24	-46	88	99
C-H coupling	85	84	-21	-37	93	98

thermodynamic parameters ΔH^\ddagger , ΔS^\ddagger and ΔG^\ddagger were then determined from the Eyring plot, $\ln(k/T)$ vs. $1/T$:

$$\ln\left(\frac{k}{T}\right) = \frac{-\Delta H^\ddagger}{R} \frac{1}{T} + \left\{ \ln\left(\frac{k_B}{h}\right) + \frac{\Delta S^\ddagger}{R} \right\} \quad (4)$$

where k_B , h and R are the Boltzmann, Planck's and gas constants, respectively. ΔH^\ddagger and ΔS^\ddagger are extracted from the slope and intercept from the plot $\ln(k/T)$ vs. $1/T$ (Figure S5, Supporting Information). The results are summarized in Table 2. When compared to non-cavity conditions, VSC on both C=O and C-H vibrations shows reduced ΔH^\ddagger and ΔS^\ddagger for cis-trans and trans-trans products. However, the relative Gibbs free energy change between the con- and disrotatory transition states is increased upon VSC on C=O (10.8 ± 0.5 kJ mol⁻¹), while it is reduced under VSC on C-H (4.9 ± 0.5 kJ mol⁻¹), when compared to non-cavity condition (7.6 ± 0.5 kJ mol⁻¹). These thermodynamic changes are represented in Figure 4 and are entirely consistent with the cavity effects discussed above, in that VSC leads to stabilizing either symmetry-allowed conrotatory or symmetry-forbidden disrotatory products depending on which C=O or C-H vibrational band is coupled.

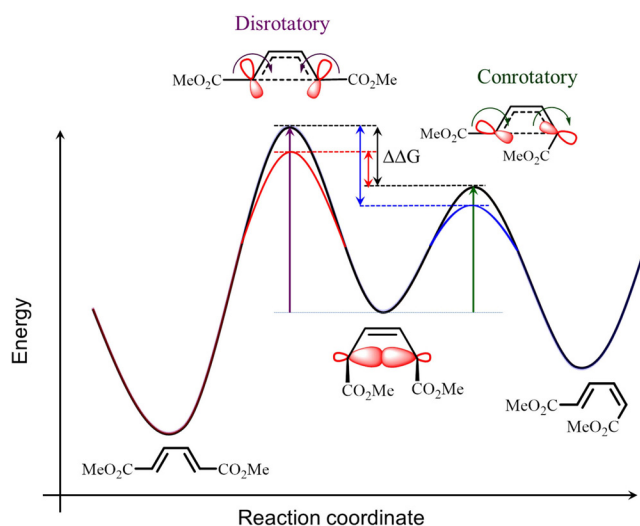


Figure 4. Energy level diagram for the con- and disrotatory electrocyclic ring-opening of CB under non-cavity and VSC conditions. The relative Gibbs free energy change ($\Delta\Delta G^\ddagger$) between symmetry-allowed conrotatory and symmetry-forbidden disrotatory transition states is altered by coupling to C=O (blue line) and C-H (red line), when compared to the non-cavity condition.

In conclusion, the modification of the stereoselectivity of a pericyclic reaction as studied here confirms the key role of symmetry in chemistry under VSC. The cavity vacuum field imposes symmetry constraints that facilitate either the con- or disrotatory pathways in such cyclic ring-opening reaction and thereby the selectivity of the Woodward–Hoffmann rules. Further such studies should enrich our understanding of the details of chemistry under VSC.

Acknowledgements

We acknowledge support of the International Center for Frontier Research in Chemistry (icFRC, Strasbourg), the ANR “ERA-NET QuantERA”—Projet “RouTe” (ANR-18-QUAN-0005-01), the ANR Equipex Union (ANR-10-EQPX-52-01), CSC (ANR-10-LABX-0026 CSC) within the Investissement d’Avenir program ANR-10-IDEX-0002-02. T.W.E. and J.M. both acknowledge the support of the ERC (project no 788482 MOLUSC and no 639170 CarbonFix, respectively). A.S. thanks the EU for a H2020 Marie Skłodowska Curie Fellowship (792101).

Conflict of interest

The authors declare no conflict of interest.

Keywords: electrocyclic ring opening · orbital symmetry · pericyclic reactions · strong coupling · Woodward–Hoffmann rules

- [1] R. B. Woodward, R. Hoffmann, *Angew. Chem. Int. Ed. Engl.* **1969**, *8*, 781–853; *Angew. Chem.* **1969**, *81*, 797–869.
- [2] P. S. Lee, S. Sakai, P. Hörstermann, W. R. Roth, E. A. Kallel, K. N. Houk, *J. Am. Chem. Soc.* **2003**, *125*, 5839–5848.
- [3] S. Niwayama, E. A. Kallel, D. C. Spellmeyer, C. Sheu, K. N. Houk, *J. Org. Chem.* **1996**, *61*, 2813–2825.
- [4] M. Yasui, Y. Naruse, S. Inagaki, *J. Org. Chem.* **2004**, *69*, 7246–7249.
- [5] M. Hasegawa, M. Murakami, *J. Org. Chem.* **2007**, *72*, 3764–3769.
- [6] T. Yoshikawa, S. Mori, M. Shindo, *J. Am. Chem. Soc.* **2009**, *131*, 2092–2093.
- [7] J. A. Hutchison, T. Schwartz, C. Genet, E. Devaux, T. W. Ebbesen, *Angew. Chem. Int. Ed.* **2012**, *51*, 1592–1596; *Angew. Chem.* **2012**, *124*, 1624–1628.
- [8] K. Hirai, J. A. Hutchison, H. Uji-i, *ChemPlusChem* **2020**, *85*, 1981–1988.
- [9] T. W. Ebbesen, *Acc. Chem. Res.* **2016**, *49*, 2403–2412.
- [10] F. Herrera, F. C. Spano, *Phys. Rev. Lett.* **2016**, *116*, 238301.
- [11] S. R. Casey, J. R. Sparks, *J. Phys. Chem. C* **2016**, *120*, 28138–28143.
- [12] Y. Pang, A. Thomas, K. Nagarajan, R. M. A. Vergauwe, K. Joseph, B. Patrahau, K. Wang, C. Genet, T. W. Ebbesen, *Angew. Chem. Int. Ed.* **2020**, *59*, 10436–10440; *Angew. Chem.* **2020**, *132*, 10522–10526.
- [13] V. N. Peters, M. O. Faruk, J. Asane, R. Alexander, D. a. A. Peters, S. Prayakara, S. Rout, M. A. Noginov, *Optica* **2019**, *6*, 318–325.
- [14] B. Munkhbat, M. Wersäll, D. G. Baranov, T. J. Antosiewicz, T. Shegai, *Sci. Adv.* **2018**, *4*, eaas9552.

- [15] A. Thomas, J. George, A. Shalabney, M. Dryzhakov, S. J. Varma, J. Moran, T. Chervy, X. Zhong, E. Devaux, C. Genet, J. A. Hutchison, T. W. Ebbesen, *Angew. Chem. Int. Ed.* **2016**, *55*, 11462–11466; *Angew. Chem.* **2016**, *128*, 11634–11638.
- [16] J. Lather, P. Bhatt, A. Thomas, T. W. Ebbesen, J. George, *Angew. Chem. Int. Ed.* **2019**, *58*, 10635–10638; *Angew. Chem.* **2019**, *131*, 10745–10748.
- [17] J. Galego, F. J. Garcia-Vidal, J. Feist, *Nat. Commun.* **2016**, *7*, 13841.
- [18] A. Mandal, P. Huo, *J. Phys. Chem. Lett.* **2019**, *10*, 5519–5529.
- [19] B. Gu, S. Mukamel, *J. Phys. Chem. Lett.* **2020**, *11*, 5555–5562.
- [20] J. Feist, J. Galego, F. J. Garcia-Vidal, *ACS Photonics* **2018**, *5*, 205–216.
- [21] R. M. A. Vergauwe, A. Thomas, K. Nagarajan, A. Shalabney, J. George, T. Chervy, M. Seidel, E. Devaux, V. Torbeev, T. W. Ebbesen, *Angew. Chem. Int. Ed.* **2019**, *58*, 15324–15328; *Angew. Chem.* **2019**, *131*, 15468–15472.
- [22] A. Thomas, L. Lethuillier-Karl, K. Nagarajan, R. M. A. Vergauwe, J. George, T. Chervy, A. Shalabney, E. Devaux, C. Genet, J. Moran, T. W. Ebbesen, *Science* **2019**, *363*, 615.
- [23] K. Hirai, R. Takeda, J. A. Hutchison, H. Uji-i, *Angew. Chem. Int. Ed.* **2020**, *59*, 5332–5335; *Angew. Chem.* **2020**, *132*, 5370–5373.
- [24] F. Herrera, J. Owrutsky, *J. Chem. Phys.* **2020**, *152*, 100902.
- [25] J. A. Campos-Gonzalez-Angulo, R. F. Ribeiro, J. Yuen-Zhou, *Nat. Commun.* **2019**, *10*, 4685.
- [26] C. Schäfer, M. Ruggenthaler, H. Appel, A. Rubio, *Proc. Natl. Acad. Sci. USA* **2019**, *116*, 4883.
- [27] M. Hertzog, M. Wang, J. Mony, K. Börjesson, *Chem. Soc. Rev.* **2019**, *48*, 937–961.
- [28] N. T. Phuc, P. Q. Trung, A. Ishizaki, *Sci. Rep.* **2020**, *10*, 7318.
- [29] I. Vurgaftman, B. S. Simpkins, A. D. Dunkelberger, J. C. Owrutsky, *J. Phys. Chem. Lett.* **2020**, *11*, 3557–3562.
- [30] J. Flick, P. Narang, *J. Chem. Phys.* **2020**, *153*, 094116.
- [31] E. Davidsson, M. Kowalewski, *J. Phys. Chem. A* **2020**, *124*, 4672–4677.
- [32] J. Fregoni, G. Granucci, E. Coccia, M. Persico, S. Corni, *Nat. Commun.* **2018**, *9*, 4688.
- [33] V. P. Zhdanov, *Chem. Phys.* **2020**, *535*, 110767.
- [34] H. Hiura, A. Shalabney, J. George, <https://doi.org/10.26434/chemrxiv.7234721.v4>, **2019**.

Manuscript received: October 6, 2020

Revised manuscript received: November 18, 2020

Accepted manuscript online: December 11, 2020

Version of record online: February 1, 2021